WELDING RESEARCH

SUPPLEMENT TO THE *WELDING JOURNAL* APRIL 2005
Sponsored by the American Welding Society and the Welding Research Council

Influence of Molybdenum on Ferritic High-Strength SMAW All-Weld-Metal Properties

As molybdenum increased, hardness, yield, and tensile strengths increased

BY E. SURIAN, M. RAMINI DE RISSONE, AND L. DE VEDIA

ABSTRACT. The investigation described in this paper is part of a long-term study on the influence of alloying elements on the mechanical properties and microstructure of high-strength SMAW electrode weld metal of the ANSI/AWS A5.5-96 E10018/11018/12018M type. The objective of this work was to study the influence of Mo variations from nominal 0 to 0.90% for an all-weld metal alloyed with C 0.05%, Ni 1.8%, and two values of Mn: 1 and 1.5% in both the as-welded and stress-relieved conditions in order to contribute to a comprehensive picture on the influence of alloying elements on high-strength weld deposits. Tensile, impact, and CTOD testing were employed to assess the mechanical properties. Full chemical and microstructural analyses were conducted and complemented with a hardness survey. It was found that as Mo increased, hardness, yield, and tensile strengths increased. The same effect was achieved with an increment of Mn. As a general tendency, Mo was deleterious for toughness for 1% Mn, but a maximum of toughness was achieved at 0.25% Mo for 1.5% Mn. Postweld heat treatment (PWHT) produced a drop in tensile properties and a benefit on toughness, especially for Mo contents up to 0.5%. Some suggestions concerning the electrode formulation to obtain an optimum combination of tensile strength and toughness are presented.

Introduction

In recent years there has been an increase in the use of medium- and high-strength structural steels leading to a requirement for adequate welding consumables for such materials. This resulted in a significant advance in electrode formulation to obtain weld deposits with high values of strength and toughness (Ref. 1). Structural safety and a tolerance to discontinuities in welded joints are obtained by imposing requirements on toughness. This is done by setting minimum Charpy V-notch levels at a specified temperature, and minimum CTOD values at the lowest design temperature (Ref. 2). The achievement of adequate CTOD values becomes increasingly difficult as the weld metal tensile strength increases. One way to obtain improved weld metal toughness is through the control of the microstructure, which requires taking into account the weld metal chemistry. It is generally accepted that acicular ferrite is the optimum microstructure for as-welded C-Mn weld metal (up to approximately 650 MPa of tensile strength), leading to an adequate combination of strength and fracture toughness at low temperature (Refs. 3, 4). Acicular ferrite has a very fine grain size and a high concentration of dislocations that are responsible for its toughness and ductility (Ref. 5). Several workers have reported that a low transition temperature can be obtained in a C-Mn weld deposit provided the proportion of acicular ferrite is maintained at a high level, and if the amount of grain boundary ferrite with aligned M-A-C is sufficiently low (Refs. 1, 2, 5, 6). At higher strength levels, obtained through increased alloying, acicular ferrite tends to be replaced by other microconstituents such as ferrite with second phases. Thus maintaining a satisfactory combination of strength and toughness requires a precise chemical composition of the weld metal.

This investigation is part of a long-term study on the influence of alloying elements on the mechanical properties and microstructure of high-strength weld metal deposited with SMAW using an electrode of the ANSI/AWS A5.5-96 E10018/11018/12018M (Ref. 7) type. Previous studies on the influence of Mn (Ref. 8), C (Ref. 9), and Cr (Refs. 10 and 11) revealed that optimum toughness was achieved with a Mn content between 1.0 and 1.4%, very low C content (less than 0.05%), Ni 2.0%, and Mo 0.30%. With higher C (up to 0.10%) and Mn (up to 1.70%), or by adding Cr (up to 0.75%), it is still possible to have good toughness values that satisfy ANSI/AWS A5.5-96 (Ref. 7) requirements, which are 27 J minimum at –51°C (–60°F). This work studied the influence of Mo variations from nominal 0 to 0.90% for an all-weld metal alloyed with C 0.05%, Ni 1.8%, and 1 and 1.5% Mn. In order to contribute to a comprehensive picture on the influence of alloying elements on high-strength weld deposits, they were studied in the as-welded (AW) and stress-relieved (SR) conditions,.

E. SURIAN is with Research Secretary, Engineering Faculty, with National University of Lomas de Zamora/Deytema, Regional Faculty San Nicolás, National Technological University, Buenos Aires, Argentina. M. RAMINI DE RISSONE is with Deytema-Material Development and Technology Center, Regional Faculty San Nicolás, National Technological University, Buenos Aires, Argentina. L. DE VEDIA is with Sabato Institute, National University of San Martín-CNEA, CIC. Buenos Aires, Argentina.

KEY WORDS

Acicular Ferrite
Heat Treatment
High-Strength Alloys
Mechanical Properties
SMAW
Toughness

Experimental Procedure

Electrodes

Eight low-hydrogen iron powder experimental electrodes were designed varying the amount of metallic molybdenum powder in the coating, in such a way as to obtain in the all-weld metal nominal 0, 0.25, 0.50, and 0.90% Mo for two values of Mn at 1 and 1.5%. Ni was maintained in 1.8% and no Cr was added. The core wire diameter was 4 mm and the coating factor

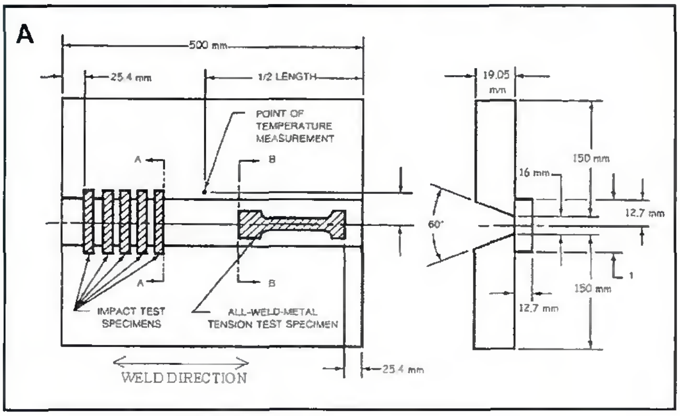

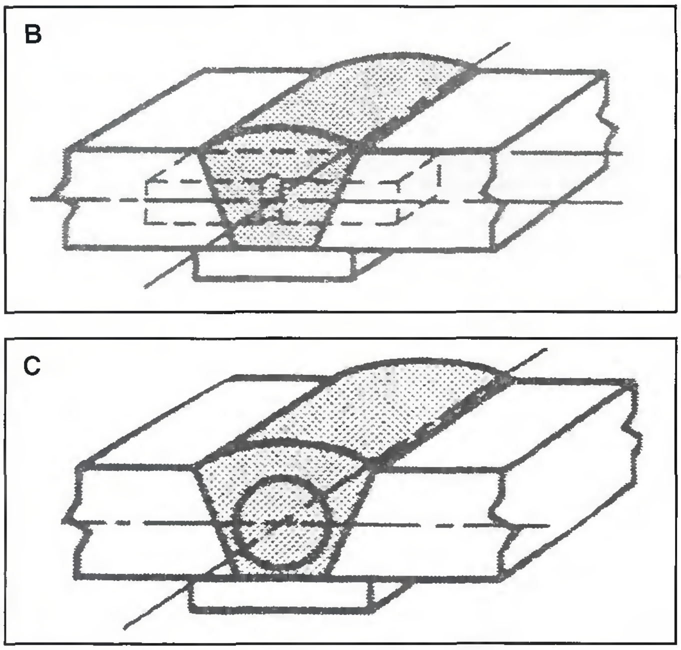

Fig. 1 — A — Test plate showing coupon design and locations of test specimens; B — location of impact test specimen and Charpy V-notch test location; C — location of all-weld-metal tension test specimen.

1.65 in all cases. To ensure identical starting conditions, the electrodes were redried for one hour at 350°C (662°F) before being used.

All-Weld-Metal Test Coupons

With each of the eight electrodes, two all-weld-metal test coupons were welded according to ANSI/AWS A5.5-96 (Ref. 7) using a carbon steel base plate of ¾ in. (19 mm) thickness — Fig. 1. Welding was performed in the flat position, changing the welding direction after each bead and using two beads per layer, except for the last layer where only one bead was deposited, but with the same heat input so as to obtain a center bead for metallographic study. No evidence of weld cracking was found. Table 1 shows the welding parameters used on all weld coupons.

Table 1 — Welding Parameters Used in ANSI/AWS A5.5-96 All-Weld-Metal Coupons

Number of layers	Number of passes	Interpass temperature (°C)	Intensity (A)	Tension (V)	Welding speed (mm/s)	Heat input (kJ/mm)
7	15	103	170	24	1.9	2.2

Mechanical Testing

After conducting an X-ray examination, the following test specimens were extracted from each test coupon (Fig. 1): minitrac (Ref. 12) specimen (total length = 55 mm, gauge length = 25 mm, reduced section diameter = 5 mm, gauge length to diameter ratio = 5:1), to measure tensile properties; a cross section to conduct a hardness survey and to perform a metallographic study; bend specimens for CTOD determination; and approximately 20 Charpy V-notch impact specimens in order to assess the absorbed energy vs. test temperature curve. All specimens were tested in the as-welded condition and after a postweld stress relief heat treatment of 1 h at 621 ± 14°C (1150 ± 25°F) (cooling rate: 100°C/h). Tensile properties were determined at room temperature after a hydrogen removal treatment at 100°C (212°F) during 24 hours, and impact energies were measured at temperatures between 20°C (68°F) and –70°C (–94°F). Vickers hardness (HV10) was measured in the top down direction along the centerline of the weld cross section — Fig. 2.

Metallographic Study

Examination of cross sections (etched with Nital 2%) was carried out in the top beads and the adjacent reheated zones as described previously (Ref. 13). The percentages of columnar and reheated zones were measured at 500× at the notch location for the Charpy test — Fig. 2. The average width of the columnar grain size (the prior austenite grains) was measured in the top bead of the samples at 100×. To quantify the microstructural constituents of the columnar zones in each weld, 10 fields of 100 points were measured in the top bead at 500× by light microscopy. The reheated fine-grain size was measured in the heat-affected zone of the top bead, according to the Linear Intercept Method (ASTM E112 standard). X-ray diffraction was employed to detect the presence of retained austenite in the columnar zone.

CTOD Testing

Fracture toughness of the as-welded and stress-relieved specimens was assessed by means of CTOD testing. For this purpose, full-thickness, single-edge-notched, three-point bend specimens were extracted from each weld, with the notch in the through-thickness direction as indicated in Fig. 3. An initiating fatigue crack, with initial crack depth-to-width ratio of a/w = 0.5, was used in all cases. In order to promote plane strain conditions at the crack tip, 25% side grooving of the specimens were adopted (Ref. 14). Testing was conducted at –10°C (14°F) according to ASTM 1820 (Ref. 15).

Results and Discussion

Chemical Composition

Table 2 shows the all-weld-metal chemical composition analysis results. It can be observed that the values for each element were fairly uniform, except for the two levels of Mn (1 and 1.5%) and the Mo, which varied systematically from 0.01 to 0.87%. Nitrogen and O contents were within the normal values for this type of electrode (Refs. 16, 17). The observed variations in the values among the different specimens were within the range accepted for this de-

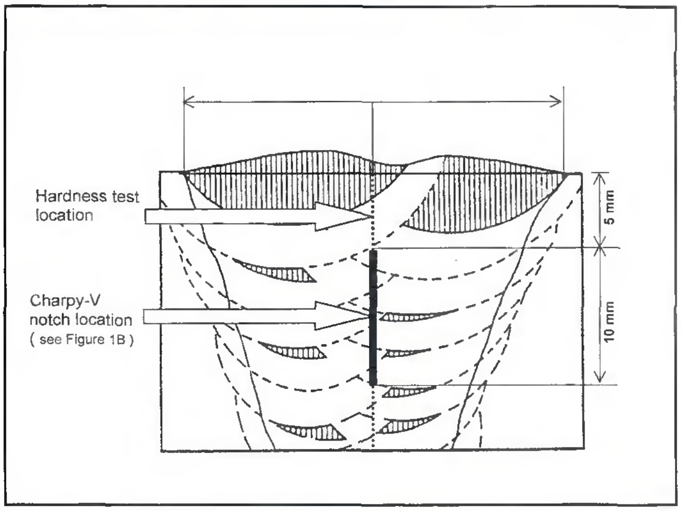

Fig. 2 — Schematic drawing of all-weld-metal test assembly cross section.

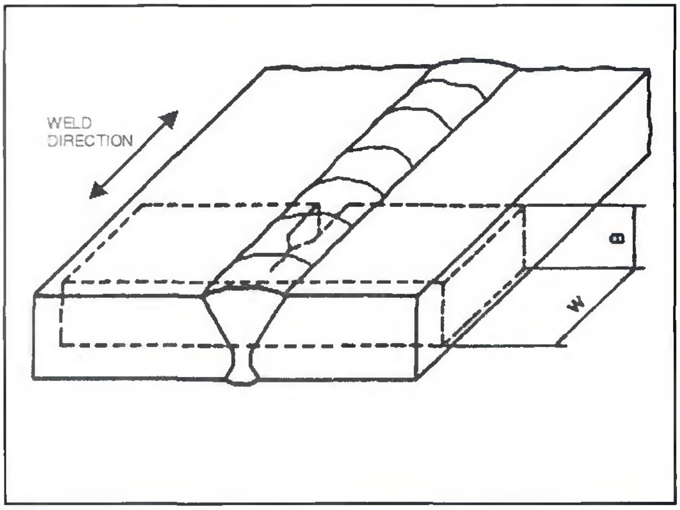

Fig. 3 — Schematic drawing of CTOD test specimen and dimensions: W and B.

Table 2 — All-Weld-Metal Chemical Composition

All weld metal samples	Element								
	C	P	S	Si	Mn	Ni	Mo	O	N
1Mn0Mo	0.06	0.012	0.009	0.37	1.03	1.93	0.01	399	107
1Mn25Mo	0.06	0.018	0.009	0.40	1.11	1.91	0.28	340	100
1Mn50Mo	0.06	0.019	0.012	0.39	1.03	1.85	0.58	406	108
1Mn90Mo	0.05	0.019	0.010	0.37	0.95	1.82	0.87	421	119
15Mn0Mo	0.05	0.018	0.009	0.58	1.54	1.87	0.01	310	95
15Mn25Mo	0.05	0.020	0.011	0.41	1.48	1.89	0.27	327	100
15Mn50Mo	0.06	0.019	0.010	0.45	1.43	1.79	0.57	398	93
15Mn90Mo	0.06	0.018	0.011	0.43	1.45	1.84	0.87	407	83

All the elements in wt-% except O and N, which are in ppm.
As, W, Co, V, Nb, Ti, and Al < 0.01%; Cu < 0.07%; Cr < 0.06%.

termination (Ref. 18). It was observed that as Mn increased, O levels decreased due to the deoxidizing effect of Mn. Increasing Mo led in general to higher oxygen values although no explanation could be advanced to account for this effect. In general, it can be observed that a "very clean" alloy base was achieved with these electrodes, with the level of residual elements being very low. Carbon values were also very low, as intended, according to previous results (Ref. 9).

Table 3 — Relative Distribution of the Columnar and Refined Regions at the Charpy V-Notch Location

All Weld Metal	Columnar Regions (%)		Refined Regions (%) Coarse Grains		Refined Regions (%) Fine Grains	
	AW	SR	AW	SR	AW	SR
1Mn0Mo	22	20	32	32	46	48
1Mn25Mo	28	27	27	27	45	46
1Mn50Mo	48	45	19	18	33	37
1Mn90Mo	54	52	15	17	31	31
15Mn0Mo	14	22	44	42	42	36
15Mn25Mo	30	30	32	31	38	39
15Mn50Mo	55	57	18	16	27	27
15Mn90Mo	59	59	16	16	25	25

Metallographic Study

General

Macrographs of multirun weldments containing 0 and 0.90% Mo and 1.5% Mn are shown in Fig. 4. They depict the observed difference in etching response (Nital 2%) on alloying, as previously found by Evans (Ref. 19). The "memory" effect quoted by Evans, which consisted of retaining the underlying columnar formation, was found in the samples with 0 to 0.90% Mo for both Mn values. However, this effect was less marked than in the case mentioned by Evans due to the fact that in the present work all the specimens contained 1.8% Ni, and that has a similar, although less strong, "memory" effect than Mo on C-Mn systems (Ref. 20).

Table 3 shows the distribution of the columnar and reheated zones along the vertical central line for the Charpy V-notch location of the all-weld-metal specimens for AW and SR conditions. It can be seen that as the Mo content increased, the percentages of columnar zones also increased. Manganese seemed to have a

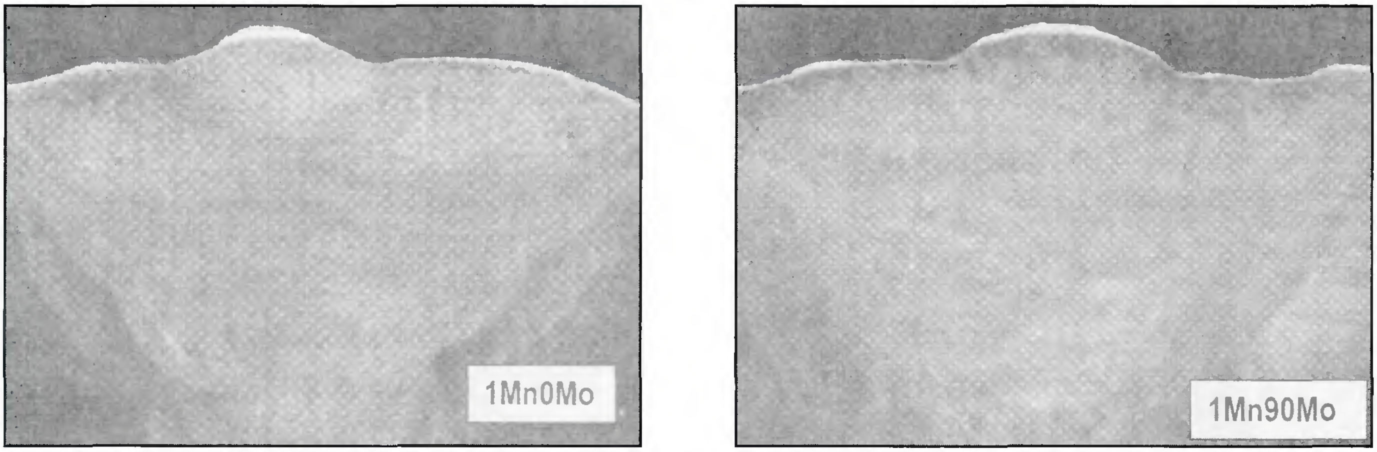

Fig. 4 — Macrophotographs of multirun deposit transverse cuts.

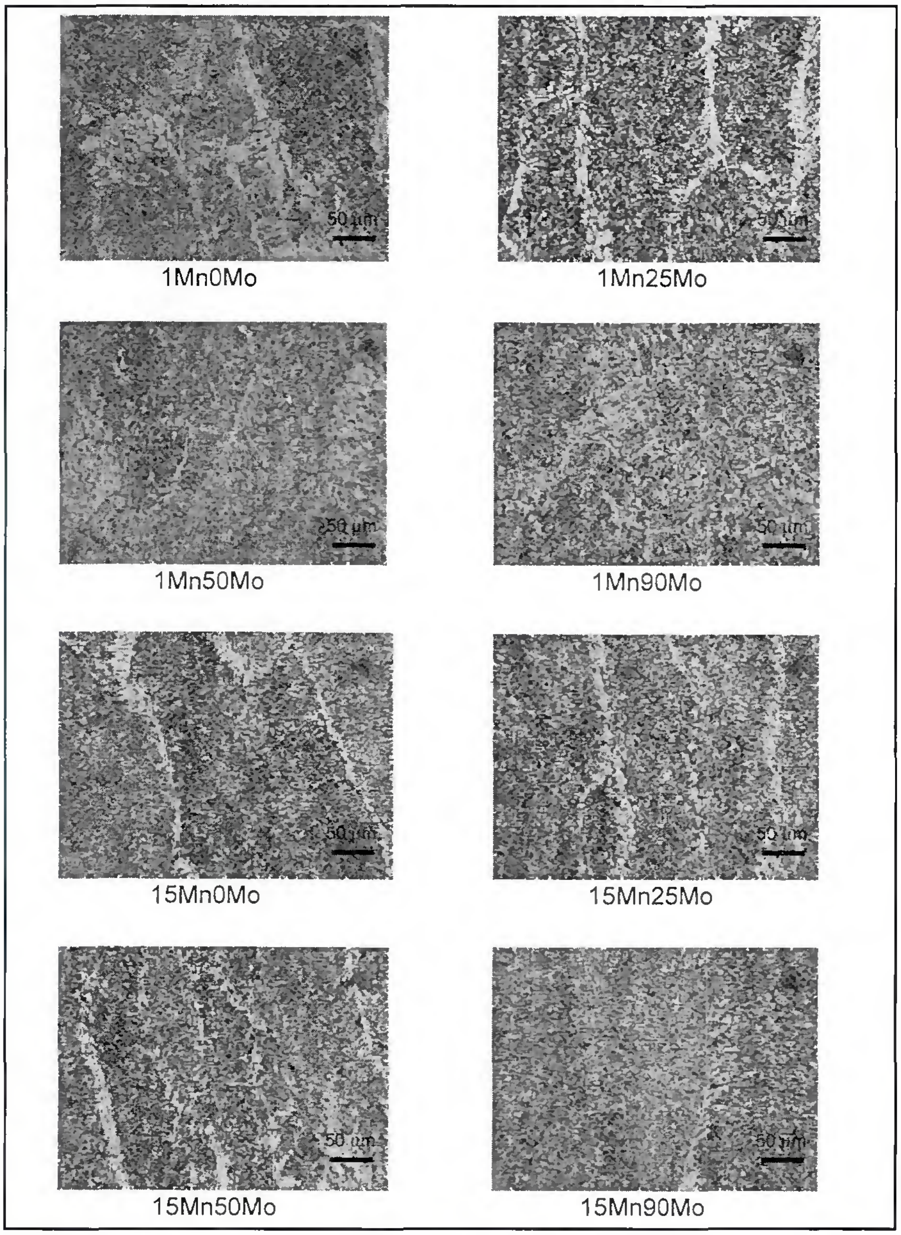

Fig. 5 — As-welded condition columnar zone microphotographs.

Table 4 — Primary Austenitic Grain Size in the Columnar Zone of the Top Bead and Fine Grain Size in the Reheated Zone

All Weld Metal	Average Columnar Grain Width (µm)	Average Reheated Fine Grain Diameter (µm)
1Mn0Mo	119	5.68
1Mn25Mo	104	5.10
1Mn50Mo	97	4.40
1Mn90Mo	85	4.02
15Mn0Mo	102	4.90
15Mn25Mo	93	4.08
15Mn50Mo	87	3.70
15Mn90Mo	78	3.58

similar but less marked effect. The percentage of coarse-grained reheated zones were lower that fine-grained zones. The described effect was found in both AW and SR test specimens, as expected.

As-Deposited Regions

The microstructure of the columnar zones for the AW condition is shown in Fig. 5. As Mo and Mn contents increased, a progressive refinement of the microstructure was observed, as described previously (Refs. 19, 21, 22), the effect of Mn is less marked. The average width of the columnar grains decreased, as shown quantitatively in Table 4, with the increment of both Mo and Mn.

Four main constituents were identified: acicular ferrite (AF), grain boundary primary ferrite PF(G), intragranular primary ferrite PF(I), and ferrite with second phase (FS). Figure 6 shows that for 1% Mn, and as Mo increased up to 0.5%, AF increased, and then decreased. This effect was produced at the expense of FS. Both PF(G) and PF(I) decreased with the in-

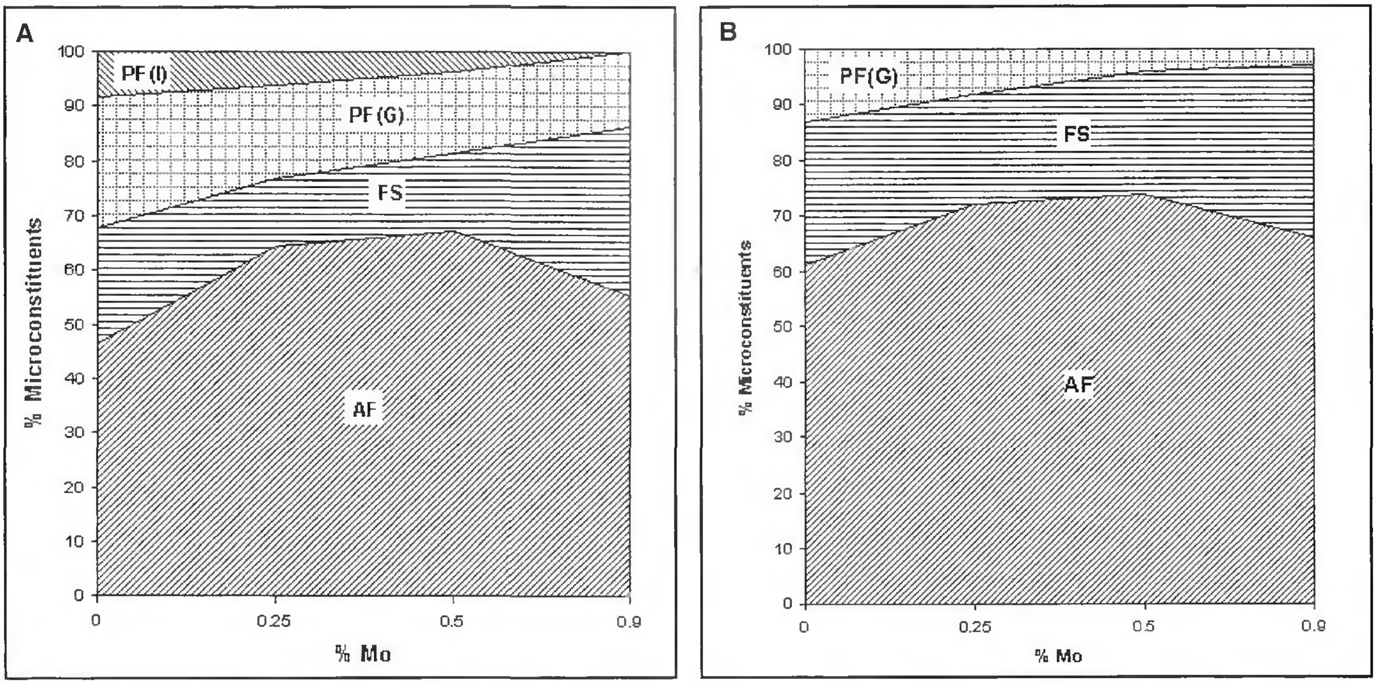

Fig. 6 — Top bead microconstituents vs. Mo content. A — 1% Mn; B — 1.5% Mn.

crement of Mo content. For 1.5% Mn, no PF(I) was measured, and the same behavior was found for 1 % Mn. Acicular ferrite increased up to 0.5% Mo, and then decreased at the expense of FS. Grain boundary primary ferrite decreased with Mo increment. The same effect was found by Evans (Ref. 19 and 21).

Reheated Zones

Table 4 also shows that with increasing Mo and Mn contents there was a progressive microstructural refinement in the reheated regions subjected to austenitizing temperature by the subsequent passes, as previously reported (Refs. 19, 21, 22). Figure 7 shows examples of the fine-grain areas for the extreme values of both Mo and Mn. Again, a general grain refinement could be observed.

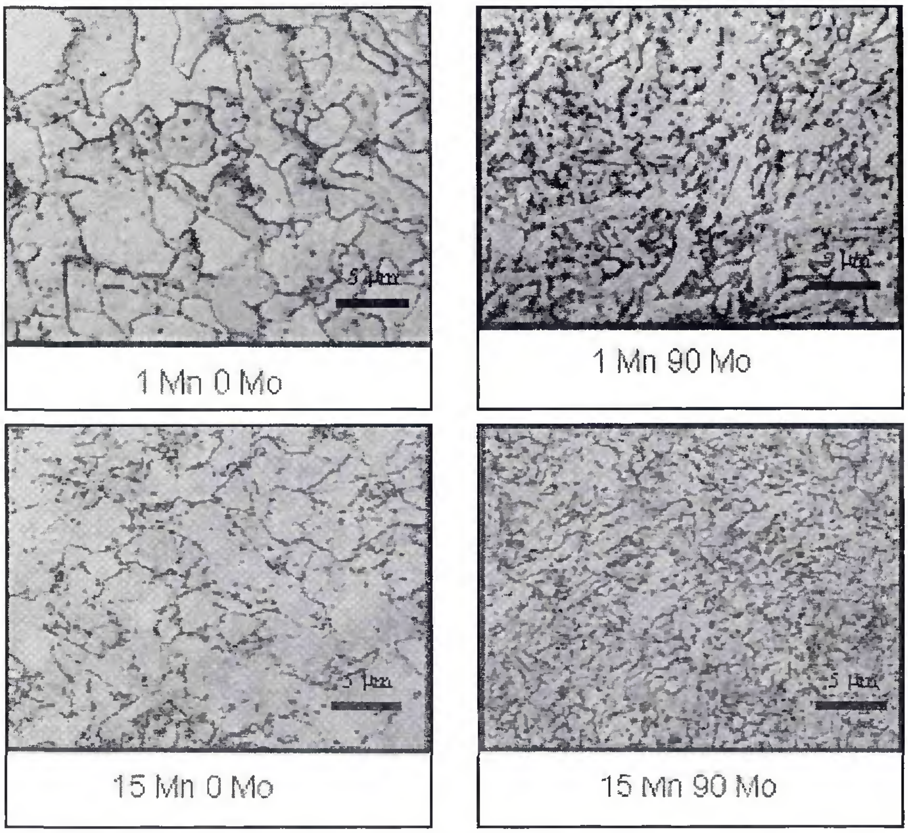

Fig. 7 — As-welded condition reheated zone microphotographs.

Retained Austenite

A small amount of retained austenite was measured in the last run columnar zone (Table 5). An increase in the amount of retained austenite was observed for higher Mn content. The maximum values for retained austenite for each Mn content was found in the absence of Mo. A minimum of retained austenite was found at 0.25% Mo, but no apparent reason was detected for this effect.

Mechanical Properties

The 18 all-weld-metal specimen radiographs were free of defects.

Hardness Survey

Table 6 shows the average values of hardness measurements in the AW and SR conditions. As expected, hardness values increased as the Mo and Mn increased in agreement with the tensile test results. Stress relieving seemed to produce a slight

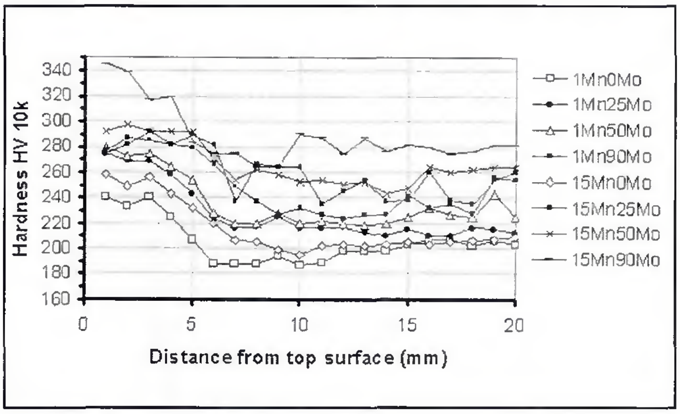

Fig. 8 — Hardness measurement results.

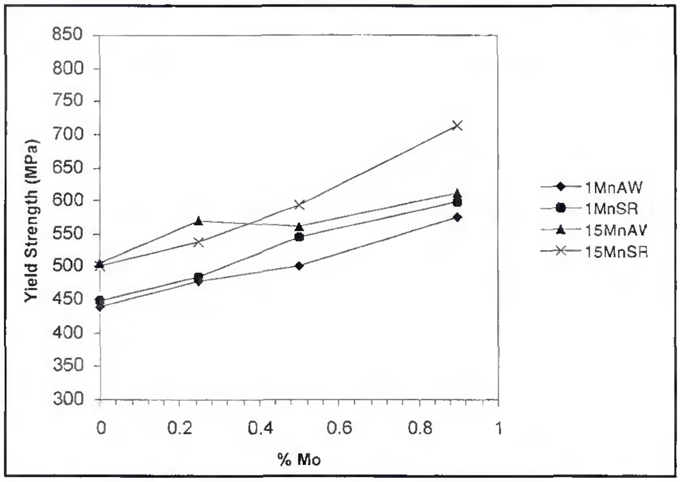

Fig. 9 — Effect of molybdenum on yield strength.

decrease in hardness for low levels of Mo and the opposite effect for Mo higher than 0.5% — Fig. 8.

All-Weld-Metal Tensile Properties

Table 6 and Figs. 9 and 10 show the tensile properties measured for AW and SR conditions. It can be seen that in all cases an increase in Mo led to increased tensile and yield stresses. For Mo contents up to 0.5%, the postweld heat treatment produced a moderate decrease in tensile values. However, this effect vanishes for higher Mo contents and even becomes reversed in the measured values for yield strength, in total accordance with the average hardness values measured. This softening effect of the stress relief heat treatment for Mo content lower than 0.5%, and hardening effect for higher Mo values, is in agreement with that reported by Evans for C-Mn ferritic deposits (Ref. 19). As expected, an increase in Mn led in all cases to a corresponding increase in tensile properties (Refs. 21, 22).

Taking into account the AWS requirements for this type of electrode (Ref. 7) (Table 7), it can be seen that the minimum tensile strength values needed for the classification of the E10018M weld metal in the as-welded condition were achieved only by the 1.0Mn-0.90Mo and 1.5Mn-0.90Mo welds, and this is with the maximum Mo levels used in this work, at least with the heat input employed in the welding of those samples. If an increase in tensile properties in these deposits was desired, it would be necessary either to reduce the heat input (Refs. 23, 24), or to increase the content of alloying elements. In this last case, taking into account the deleterious effect of increasing Mo (Ref. 19) and an excess of Cr (Refs. 10, 25, and 26), the content of this element should be adjusted for a specific Mo level like, for example, that found as optimum in this work for 1.5% Mn and 0.25% Mo. This is what is being done in this type of ferritic deposits in order to obtain electrodes classified as E11018M and E12018M (Refs. 27–30).

All-Weld-Metal Charpy V-Notch Impact Properties

The individual Charpy V-notch impact values and the calculated averages for different test temperatures obtained from the eight coupons are given in Table 8, in the as-welded and stress-relieved conditions, respectively. Values comfortably in excess of the minimum ANSI/AWS A5.5-96 requirements, 27 J at –51°C (–60°F),

Table 5 — Percentages of Retained Austenite in the Last Bead Columnar Zone, Analyzed by X-ray

Retained Austenite (%)							
1Mn0Mo	1Mn25Mo	1Mn50Mo	1Mn90Mo	15Mn0Mo	15Mn25Mo	15Mn50Mo	15Mn90Mo
0.01185	0.00278	0.00668	0.00723	0.01500	0.00834	0.01542	0.02688

Table 6 — All-Weld-Metat Tensile Property and Hardness Measurements

As-Welded Condition								
Property	1Mn0Mo	1Mn25Mo	1Mn50Mo	1Mn90Mo	15Mn0Mo	15Mn25Mo	15Mn50Mo	15Mn90Mo
TS (MPa)	515	557	604	652	607	639	657	760
YS (MPa)	438	477	500	575	505	570	562	611
E (%)	36.6	28	30.4	25.0	32.6	25.8	26.6	22.0
Hardness(a)	205	227	236	259	215	249	266	288
Stress-Relieved Condition								
Property	1Mn0Mo	1Mn25Mo	1Mn50Mo	1Mn90Mo	15Mn0Mo	15Mn25Mo	15Mn50Mo	15Mn90Mo
TS (MPa)	476	531	600	660	558	600	652	738
YS (MPa)	447	486	545	598	500	537	593	714
E (%)	35.2	33.4	28.6	25.6	30.0	29.0	23.8	22.2
Hardness(a)	180	216	248	267	201	242	268	294

(a) Average Vickers 10-kg measurements.

were achieved with all the assemblies at the mentioned temperature. The average values were similar to those obtained with commercial E100/110/12018M type electrodes (Refs. 23, 24). Figures 11 and 12 show the curves of absorbed energy vs. test temperature for each group of electrodes corresponding to both Mn contents and both AW and SR conditions. It can be observed that for 1% Mn, Mo between 0 and 0.9% had a deleterious effect on toughness in both AW and SR conditions. The PWHT produced an improvement in toughness that decreased as Mo increased and disappeared for 0.9% Mo. For 1.5% Mn in the AW condition, the best impact values were achieved with 0.25% Mo. In this case, the PWHT had a beneficial effect on toughness, especially for low Mo contents. For Mo higher than 0.25%, toughness markedly deteriorated in both AW and SR conditions. All these effects can be seen in Fig. 13, which comparatively shows the transition temperatures for 100 J of absorbed energy.

Impact values corresponding to 1% Mn were, as a general tendency, larger than those of 1.5% Mn, but this difference became smaller as the Mo content increased. Evans (Ref. 19) detected an optimum for 0.25% Mo in C-Mn ferritic deposits in the AW condition, for Mn content of 1.0%; this optimum disappeared for higher Mn values. In the present work, no such maximum was found for 1% Mn, since impact toughness deteriorated continuously as Mo increased. A relative maximum of toughness was found for 1.5% Mn at 0.25% Mo. This change in the Mn content for which a relative maximum was obtained in this work could be due to the presence of 1.8% Ni. Coincidently with Evans (Ref. 19) for PWHT deposits, Mo was deleterious for toughness, especially for values higher than 0.5%.

Considering the AWS Charpy V-notch requirement of 27 J at –51°C (–60°F) in the as-welded condition, there was not a single value below this requirement. However, for this type of material, the consumable producer commercial catalogs (Refs. 27–30) report toughness around 50 J at –51°C. Then, to obtain the adequate tensile properties without compromising toughness values, Mo content should be maintained not higher than 0.25%. This conclusion allows to compromise the all-weld-metal Mo content required by ANSI/AWS A5.5-96 for E100/110/12018M electrodes, of 0.25 to 0.50% for the two first classifications and 0.30 to 0.55% for the last one, with the optimum Mo level for this system.

CTOD Results

In Table 9 and Fig. 14A and B, average CTOD test results corresponding to the full thickness specimens extracted from the all-weld-metal welds are shown for the AW and SR conditions. A general trend toward decreasing CTOD values with increasing Mo content was observed, for both conditions. The same deleterious effect was obtained with Mn, as previously found (Ref. 8) in a similar alloying system. PWHT led to an improvement in fracture toughness

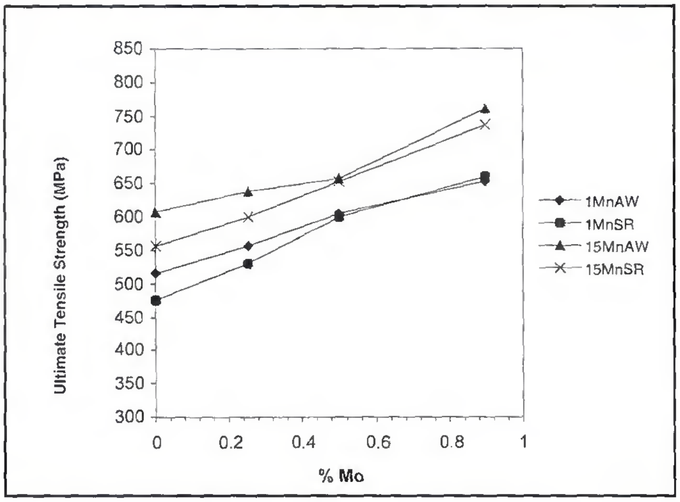

Fig. 10 — Effect of molybdenum on ultimate tensile strength.

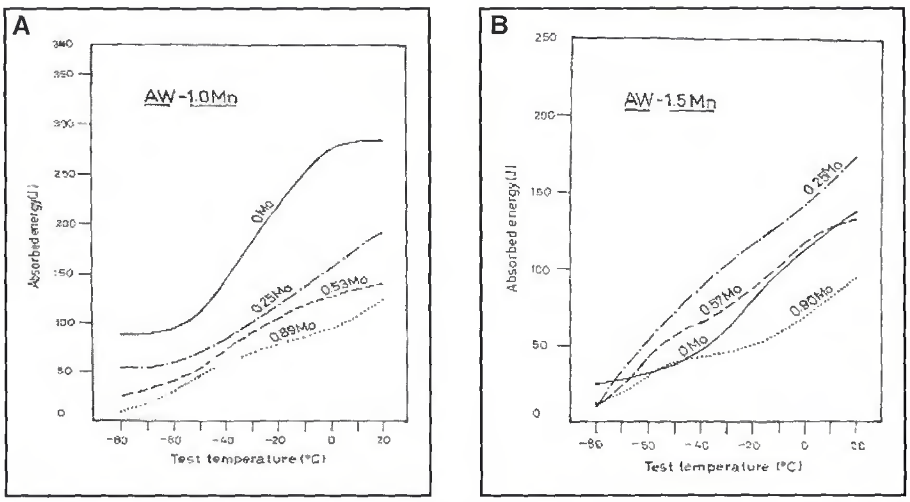

Fig. 11 — Charpy V-notch impact results for all-weld metals in the as-welded condition. A — 1% Mn; B — 1.5% Mn.

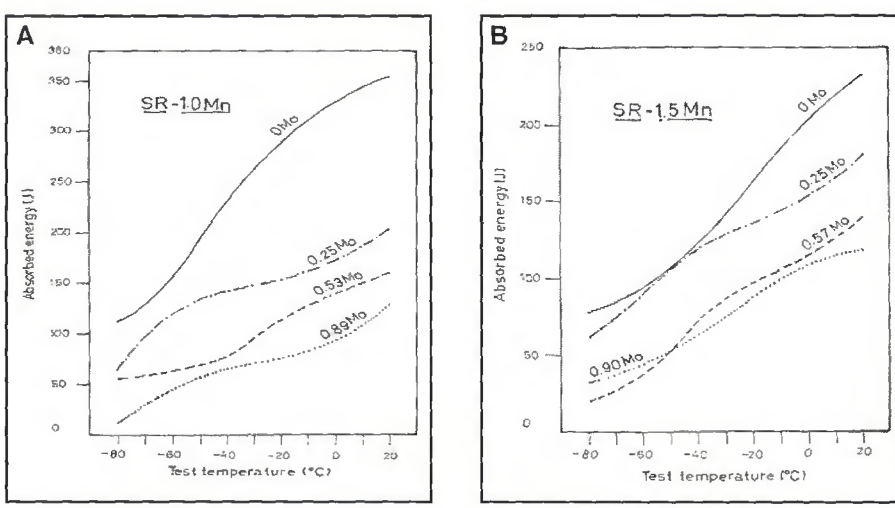

Fig. 12 — Charpy V-notch impact results for all-weld metals in the stress relief condition. A — 1% Mn; B — 1.5% Mn.

for Mo up to 0.5% with 1% of Mn, and up to 0.25% for 1.5% Mn in general agreement with the trend found in impact, hardness, and tensile test results.

Final Remarks

The literature (Refs. 8–10, 23, 24, 31, 32) has shown that in the high-strength, low-alloy ferritic system, the problem is not so much good toughness but to achieve adequate tensile strength levels to satisfy the requirements in the relevant standards. Additionally, these materials are very sensitive to heat input (Refs. 23, 24, 31) and the guidelines to produce the all-weld metal test coupons for mechanical properties determination allow for ample procedure variations (Refs. 7, 33, 34). On the other side, for deposits of the same type (high-strength C-Mn-Ni-Mo and C-Mn-Ni-Mo-Cr low-alloy weld deposits) obtained by different welding processes (SMAW, FCAW, MCAW, and SAW), the tensile requirements of the relevant standards differ. For SMAW the range of yield strength values are specified along with minimum tensile strength, while for FCAW, MCAW, and SAW minimum values of yield strength and a range for tensile strength values are given (Refs. 7, 33 and 34). Thus, a stringent welding procedure must be defined within the limits imposed by the corresponding AWS standard in order to ensure repeatability of the resulting tensile properties of a given weld metal in this system.

Table 7 — AWS Tensile Property Requirement

	As-Welded Condition		
Property	E10018M	E11018M	E12018M
TS (MPa)	690	760	830
YS (MPa)	610–690	680–760	745-830
E (%)	20	20	18

Table 8 — All-Weld Metal Charpy-V Impact Values

As-Welded Condition								
T (°C)	1Mn0Mo	1Mn25Mo	1Mn50Mo	1Mn90Mo	15Mn0Mo	15Mn25Mo	15Mn50Mo	15MN90Mo
20	336-234 285	188-194 191	136-150 143	120-132 126	134-140 137	168-176 172	132	116
0	318-234 276	140-132 136	142-112 127	110-75 93	118-118 118	146-134 140	116	109
–20	184-184 184	136-134 135	110-94 102	88-64 76	60-86 73	108-110 109	80-94 87	82-80 81
–30	197-157-194 183	91-93-85 90	87-81-81 83	77-70-61 69	55-63-59 59	114-89-105 103	75-70-66 70	76-76-68 73
–40	158-150-90 133	97-97-83 92	80-68-75 74	60-55-70 62	40--50-55 48	90-83-90 88	71-71-70 71	60-54-58 58
–50	139-116-89 115	55-81-82 73	36-57-55 49	42-88-57 62	27-26-27 27	90-63-60 71	34-61-61 52	60-38-56 51
–60	77-102-104 94	47-73-57 59	36-50-43 43	40-62-44 49	25-44-55 41	47-69-45 54	40-59-47 49	48-50-93 49
–70	77-103 90	52-60 56	37-27 32	36-24 30	12-13 13	25-30 28	27-21 24	30-40 35
Stress-Relieved Condition								
T (°C)	1Mn0Mo	1Mn25Mo	1Mn50Mo	1Mn90Mo	15Mn0Mo	15Mn25Mo	15Mn50Mo	15MN90Mo
20	356-344 350	198	156-158 157	120-132 126	230	168-190 179	132	116
0	352-272 312	174-158 166	132-132-132 132	110-76 93	178-190 184	156-144 150	120-102 111	109
–20	269-289 279	160-160 160	108-116 112	8-64 76	146-140 143	143-121 132	90-96 93	82-80 81
–30	232-249-239 240	153-150-150 151	92-65-85 81	77-70-61 69	130-130-146 135	136-101-123 120	84-99-82 88	76-76-68 73
–40	224-234-174 211	139-144-128 137	83-65-90 79	60-55-70 62	158-129-126 138	129-120-108 119	82-32-53 56	60-54-60 58
–50	178-203-26 202	144-124-127 12	55-60-62 59	42-88-57 62	120-114-130 121	120-101-102 108	59-66-70 65	60-38-56 51
–60	124-176-175 158	124-108-128 120	64-62-57 61	40-62-44 49	96-88-74 86	75-88-70 78	35-32-17 28	48-50-93 64
–70	140-144 142	100-67 84	48-72 60	35-24 30	81-95 88	77-91 84	30-34 32	30-41 36

Table 9 — All-Weld Metal CTOD Values

	Critical Displacement δ_c (mm)							
Condition	Mn0Mo	1Mn25Mo	1Mn50Mo	1Mn90Mo	15Mn0Mo	15Mn25Mo	15Mn50Mo	15MN90Mo
AW	1.22	0.73	0.44	0.35	0.77	0.39	0.34	0.24
SR	1.30	1.01	0.53	0.22	0.80	0.57	0.17	0.07

Conclusions

When Mo content was increased from 0 to 0.9%, for Mn contents of 1 and 1.5%, in 1.8%Ni, Cr-free ferritic all-weld metal, the following was found:

1) As Mn increased, O levels decreased due to the deoxidizing effect of Mn. Increasing Mo led in general to higher oxygen values, although no explanation could be advanced to account for this effect.

2) As the Mo content increased, the percentages of columnar zones also increased. Manganese seemed to have a similar but less marked effect. Coarse-grained reheated zones were lower that fine-grained zones.

3) As Mo and Mn contents increased, a progressive refinement of the microstructure was observed in the columnar regions, with the effect of Mn less marked. The average width of the columnar grains decreased with the increment of both Mo and Mn. For 1% Mn and as Mo increased, AF increased up to 0.5% Mo and then decreased. This effect was produced at the expense of FS. Both PF(G) and PF(I) decreased with the increment of Mo content. For 1.5% Mn, no PF(I) was measured and the same behavior was found for 1% Mn. Acicular ferrite increased up to 0.5% Mo and then decreased at the expense of FS. Granular primary ferrite decreased with Mo increment.

4) As a result of the increasing Mo and Mn contents, there was also a progressive microstructural refinement in the reheated regions subjected to austenitizing temperature by the subsequent passes.

5) Small amounts of retained austenite were measured in the last run columnar zone. An increase in the amount of retained austenite was observed for higher Mn content.

6) Hardness values increased as the Mo and Mn increased in agreement with the tensile test results. Stress relieving seemed to have produced a slight decrease in hardness for low levels of Mo and the opposite effect for Mo higher than 0.5%.

7) In all cases, an increase in Mo led to increased tensile and yield stresses. For Mo content up to 0.5%, the postweld heat treatment produced a moderate decrease in these values. However, this effect vanishes for higher Mo contents and even becomes reversed in the measured values of yield strength, in total accordance with the average hardness values measured. As expected, an increase in Mn led in all cases to a corresponding increase in tensile properties.

8) Values comfortably in excess of the minimum ANSI/AWS A5.5-96 requirements of 27 J at –51°C (–60°F) were achieved with all the assemblies. The average values were similar to those obtained with commercial E100/110/12018M electrodes. For 1% Mn, Mo between 0 and 0.9% had a deleterious effect on toughness in both AW and SR conditions. The PWHT produced an improvement in toughness that decreased as Mo increased and disappeared for 0.9% Mo. For 1.5% Mn, in the AW condition the best impact values were achieved with 0.25% Mo. In this case, the PWHT had a beneficial effect on toughness, especially for low Mo contents. For Mo higher than 0.25%, toughness markedly deteriorated in both AW and SR conditions.

9) Impact values corresponding to 1% Mn were as a general tendency larger than those of 1.5% Mn, but this difference became smaller as the Mo content increased.

10) A relative maximum of toughness was found for 1.5% Mn at 0.25% Mo.

11) A general trend toward decreasing CTOD values with increasing Mo content was observed, for both AW and SR conditions. The same deleterious effect was ob-

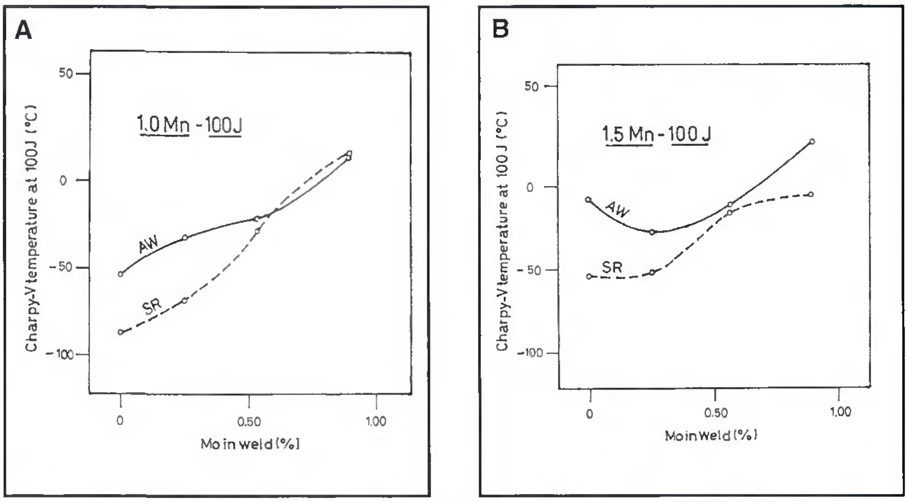

Fig. 13 — Test temperature for 100 J absorbed energy. A — 1% Mn; B — 1.5% Mn.

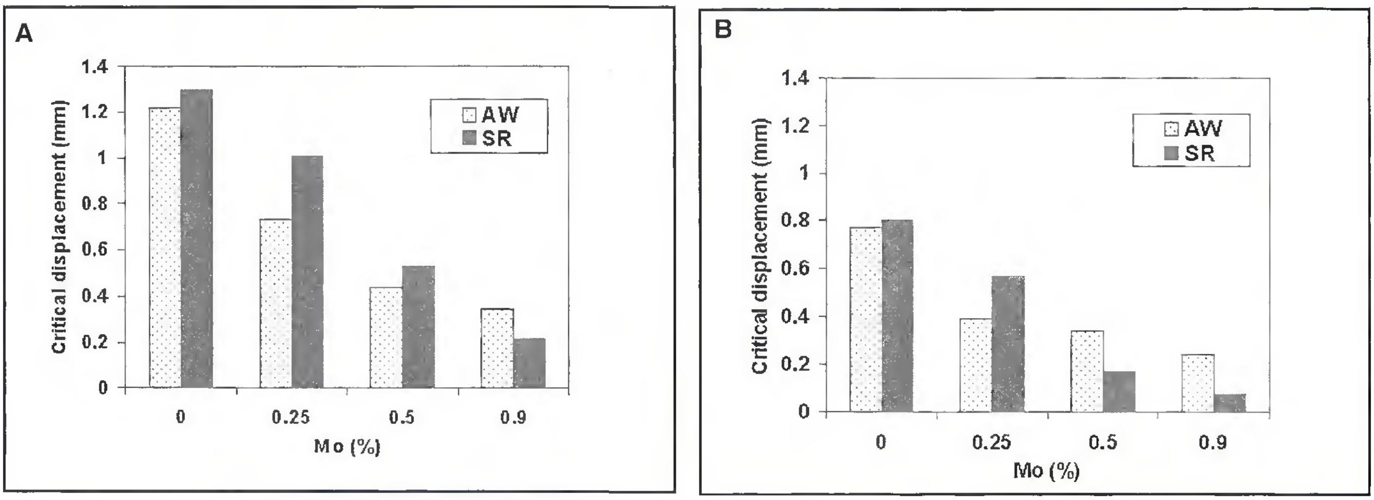

Fig. 14 — CTOD test results: A — 1 % Mn; B — 1.5 % Mn.

tained with Mn variation. Postweld heat treatment led to an improvement in fracture toughness for Mo up to 0.5% with 1% of Mn, and up to 0.25% for 1.5% Mn, which is in general agreement with the trend found in impact, hardness, and tensile test results.

Acknowledgments

The authors wish to express their gratitude to Conarco Alambres y Soldaduras SA for the fabrication of the experimental electrodes, to Air Liquide Argentina SA for the facilities to weld the test specimens, to Fundación Latinoamericana de Soldadura for the facilities to weld and to perform mechanical testing, and to ANPCyT, Argentina, for the funding support. They are also very grateful to Eng. Edmundo Tolabin, Jujuy National University, Argentina, for carrying out the metallographic study and the supervision of mechanical testing.

References

1. George, M., Still, J., and Terry, P. 1981. Gas metal arc welds for high toughness applications — microstructure and other factors. *Metal Construction* 13(12): 730–737.

2. Keeler, T. 1981. Innershield welding, part 1 — development and applications. *Metal Construction* 13(11): 667–673.

3. Garland, J. C., and Kirkwood, P. R. 1975. Towards improved submerged arc weld metal — part 1. *Metal Construction* 7(5): 275–283.

4. Garland, J. C., and Kirkwood, P. R. 1975. Towards improved submerged arc weld metal — part 2. *Metal Construction* 7 (5): 320–330.

5. Pickering, F. B. 1978. *Physical Metallurgy and the Design of Steels.* Materials Science Series, London: Applied Science Publishers.

6. Abe, N., Kitada, T., and Miyata, S. 1980. Effects of alloying elements on the toughness and microstructure of high current density gas shielded arc process weld metals. *Transact. of the JWS*, 11(4): 29–34.

7. ANSI/AWS A5.5-96, *Specification for Low-Alloy Steel Electrodes for Shielded Metal Arc Welding.* Miami, Fla.: American Welding Society.

8. Surian, E., Trotti, J., Cassanelli, A. N, and de Vedia, L. 1987. Influence of Mn content on mechanical properties and microstructure of a high strength SMA electrode weld metal. IIW-IIS Doc. II-A-724-87.

9. Surian, E., Trotti, J., Herrera, R., and de Vedia, L. A. 1991. Influence of C on mechanical properties and microstructure of weld metal from a high-strength SMA electrode. *Welding Journal* 70(6): 133-s to 140-s.

10. Surian, E., Trotti, J., Cassanelli, L. A., and de Vedia, L. A. 1994. Influence of chromium on mechanical properties and microstructure of weld metal from a high strength SMA electrode. IIW-IIS Doc. II-1204-92. *Welding Journal* 73(3): 45-s to 53-s.

11. Bott, I. de S., Souza, L., Jorge, J., and Surian, E. Microstructural evaluation of a high strength weld metal with varying Cr content by means of scanning electron microscopy. IIW-IIS Doc. II-A-936-94.

12. Schnadt, H. M., and Leinhard, E. W. 1963. Experimental investigation of the sharp-notch behavior of 60 steels at different temperature and strain rates. 1963. IIW-IIS Doc. 196-343-63.

13. Guide to the light microscope examination of ferrite steel weld metals. IIW Doc. IX-1533-88.

14. Gordon, J. R. 1985. The Welding Institute procedure for the determination of the fracture resistance of fully ductile metals. The Welding Institute Research Report, p. 275.

15. *Standard Test Method for Measurement of Fracture Toughness*, ASTM E 1820-96.

16. Blake, P. D. 1979. Nitrogen in weld metals. *Metal Construction*, April.

17. Boniszewski, T. 1992. *Self-Shielded Arc Welding.* (Tables 2.1 and 2.2), Cambridge, England: Abington Publishing.

18. Raiter, V., and Timerman, R. 1985. Chemical analysis of N and O in weld metal, round robin Test. IIW Doc. II-10459-85.

19. Evans, G. M. 1988. The influence of molybdenum on the microstructure and properties of C-Mn all-weld-metal deposits. *Join. Mat.* 1(5): 239-s to 246-s.

20. Evans, G. 1991. The effect of nickel on the microstructure and properties of C-Mn all-weld metal deposits. *Joining Sciences* 1(1): 2-s to 13-s; *Welding Research Abroad* 37(2/3): 70–83, IIW Doc. IIA-791-89.

21. Evans, G. 1980. Effect of manganese on the microstructure and properties of all-weld metal deposits. IIW Doc. II-A-432-77. *Welding Journal* 59(3): 67-s to 75-s.

22. Surian, E., and Boniszewski, T. 1992. Effect of manganese and type of current on the properties and microstructure of all-weld-metal deposited with E7016-1 electrodes. *Welding Journal* 71(9): 348-s.

23. Vercesi, J., and Surian, E. 1996. The effect of welding parameters on high-strength SMAW all-weld-metal, part 1: AWS E11018M. IIS-IIW Doc II-A-915-94. *Welding Journal* 75(6): 191-s to 196-s.

24. Vercesi, J., and Surian, E. 1997. The effect of welding parameters on high-strength SMAW all-weld-metal, part 2: AWS E10018M and E12018M. IIW-IIS Doc II-A-934-94. *Welding Journal* 77(4): 164-s to 171-s.

25. Evans, G. M. 1989. The effect of chromium on the microstructure and properties of C-Mn all-weld-metal deposits. *Weld. Met. Fab.* 57(7): 346–358.

26. Jorge, J. C. F., Souza, L. F. G., Rebello, J. M. A., and Evans, G. M. 1994. Effect of chromium on the microstructure/toughness relationship in C-Mn-Mo weld deposits. IIW/IIS Doc. II-A-930-94.

27. Catalog of Conarco manual electrodes (F-C-CO-001-001).

28. Welding consumables ESAB SeAH Corp., catalog SS-03-E, Rev. 7, 0101.

29. SAF welding consumable catalog, edition 2000.

30. Welding consumables catalog, Kobe Steel, Kobelco.

31. Surian, E., and Vercesi, J. 1997. The effect of heat input on all-weld metal mechanical properties of AWS A5.29-80 EXXXT5-K3/K4 types flux cored wires. Presented at the Professional Program, AWS Show and Annual Convention, Los Angeles, Calif.

32. Ramini de Rissone, M., Svoboda, H., Surian, E., and Vedia, L. 2004. Influence of procedure variables on C-Mn-Ni-Mo metal cored wire ferritic all-weld metal. Presented at the Professional Program, AWS Annual Convention, Chicago, Ill.

33. ANSI/AWS A5.5-96, *Specification for Low-Alloy Steel Electrodes for Shielded Metal Arc Welding.* Miami, Fla.: American Welding Society.

34. ANSI/AWS A5.23-97, *Specification for Low-Alloy Steel Electrodes and Fluxes for Submerged Arc Welding.* Miami, Fla.: American Welding Society.